Pharmacokinetic Appraisal of Carprofen Delivery from Intra-Articular Nanoparticles: A Population Modeling Approach in Rabbits [†]

Alexander Parra-Coca [1,2], Antonio Boix-Montañés [1,*], Ana Calpena-Campmany [1,3] and Helena Colom-Codina [1]

[1] Department of Pharmacy and Pharmaceutical Technology and Physical-Chemistry, Faculty of Pharmacy and Food Sciences, University of Barcelona, 08007 Barcelona, Spain; email1@gmail.com (A.P.-C.); anacalpena@ub.edu (A.C.-C.); email2@gmail.com (H.C.-C.)

[2] Department of Veterinary Medicine and Zootechnic, Faculty of Agricultural Sciences, University of Applied and Environmental Sciences (U.D.C.A.), Bogotá, Colombia

[3] Institute of Nanoscience and Nanotechnology (IN2UB), Faculty of Pharmacy and Food Sciences, University of Barcelona, 08028 Barcelona, Spain

[*] Correspondence: antoniboix@ub.edu; Tel.: +34-93-402-45-60

[†] Presented at the 1st International Electronic Conference on Pharmaceutics, 1–15 December 2020; Available online: https://iecp2020.sciforum.net/.

Abstract: Osteoarthritis is frequently treated in veterinary with non-steroidal anti-inflammatory drugs such as carprofen (CP). The enhancement of its action over the articular cartilage can be achieved by increasing drug uptake into the cartilage, alongside its site of action, and anticipating its rapid distribution towards bloodstream. A pharmacokinetic study to evaluate carprofen nanoparticles (NP) after intraarticular administration (IA) in rabbits has been performed through a modeling allometric approach. The pharmacokinetic analysis of plasma profiles showed a rapid CP distribution outwards synovial chamber but mainly remaining in plasma (Vc = 0.14 L/5 Kg), according to its high protein-binding. The absorption data modeling showed the occurrence of two different release-absorption rate processes after nanoparticles administration in the synovial space, i.e., a fast rate process causing a burst effect and involving the 59.5% of the total CP absorbed amount and a slow rate process, involving the 40.5%. Interestingly, the CP burst effect inside the joint space enhances its diffusion towards cartilage resulting in CP accumulation about three times higher concentrations than in plasma. In line with these results, the normalised-by-dose AUC values after IA administration were 80% lower than those observed after the intravenous. Moreover, the slower slope of the concentration-time terminal phase after IA administration vs. IV suggested a flip-flop phenomenon (0.35 h-1 vs. 0.19 h-1). Of note, CP clearances are predictive of the PK profile of CP in healthy humans (0.14 L/h/5 Kg vs. 2.92 L/h/70 Kg) although an over-estimation has been detected for cats or dogs (10 times and 4 times respectively). This fact could probably be attributed to inter-species metabolic differences. In summary, despite the limited number of animals used, this study shows that the rabbit model could be suitable for a predictive evaluation of the release enhancement of CP-NP towards the biophase in arthritic diseases not due to sterical retention of the formulation.

Keywords: alometric; carprofen; intraarticular; nanoparticles; non-linear-mixed-effects modelling; pharmacokinetics; PLGA-P188

1. Introduction

Osteoarthritis is managed with COX or fosfolipase A2 inhibitors to decrease prostaglandin mediators. Carprofen (CP) is a anti-inflammatory, analgesic and antipyretic propionic acid-

derivative, used in veterinary medicine [1] as alternative to corticosteroidic management of local inflammations [2]. Intraarticular administration (IA), improves local action and reduces systemic effects. Drug delivery to synovial fluid lining with the biophase, i.e., articular cartilage surface [3] improves the quality of life of animals with inflammatory arthropaties [4]. Drug uptake to the cartilage requires high synovial fluid concentrations, anticipating its rapid distribution towards bloodstream [5] due to the thin layer of specialized cells of the synovial cavity that facilitates the drug diffusion through. Indeed, a rapid equilibrium is achieved between synovial fluid and plasma [5]. Nanoparticle formulations, using biocompatible [6] Poly lactic-co-glycolic acid (PLGA) polymers, are promising [7–10] to extend the drug residence times, bioavailability and duration of effects [4]. The aim of the current study is the in vivo evaluation of CP nanoparticles for IA administration through a modelling approach, in rabbits.

2. Experiments

2.1. Reagents and Substances and Assay Solutions

Carprofen was purchased from Sigma-Aldrich. KH_2PO_4, $Na_2HPO_4.2H_2O$, acetonitrile, methanol, ortophosphoric acid 85%, sodium acetate trihydrate and ammonium acetate were purchased from Panreac (Barcelona, Spain). Deionized water (>10 MΩ.cm) was obtained on-site. Buffers were prepared as described elsewhere [11]. Poly Lactic-co-Glycolic Acid (Resomer® RG 753 S) was purchased from SigmaAldrich and Ethylene-Propylene Oxides Block Copolymer (Lutrol F68®P188) was a gift sample from Basf (Barcelona, Spain). All other reagents were also of analytical grade.

2.2. Animals and Drug Administration

Study protocol was approved (Ref.2015_089) by the animal welfare committee (Department of Agriculture, Livestock and Fisheries, 1997). Three 7-month–old white New-Zealand healthy male rabbits (Harlan, Barcelona, Spain) weighting 3.76–3.94 kg housed under standard conditions receiving food and water *ad libitum*. After anesthesia with xylazine (Rompun® 20 mg/mL, BayerHispania, Spain) and ketamine (Imalgene® 100 mg/mL, Merial, Spain), a dilution of CP Rimadyl® 50 mg/mL (Zoetis, Spain) in physiologic saline (1:1 *v/v*) was administered through the right ear vein at 4 mg/kg. Secondly, CP nanoparticles 4.5 mg/mL were administered intraarticularly at 0.5 mg/kg through the right knee joint according to a cross-over design with 7 days wash-out. The left ear vein was catheterized (22G × 1.00in., Henry Schein) and Vacutainer® tube K2E for sampling (Beckton&Dickinson, Spain).

2.3. Sampling Procedures

EDTA blood samples (1.3 mL) were always collected at 0, 0.25, 0.5, 1, 2, 4, 6, 8, 24, 48, 72 and 96 h and cooled on ice (30 min). After centrifugation (5000 rpm/10 min), plasma was stored at −80 °C until analysis. 96 h after IA administration, animals were sacrificed with pentobarbital (Dolethal® 200 mg/mL, Vetoquinol, Spain) through the auricular vein. Knees (lateral and contralateral) of one animal were excised to obtain synovial liquid, femoral articular cartilage (both condyles) and meniscus tissue. Samples were weighted in glass vials and frozen at −80 °C until analysis.

2.4. Analysis of CP in Plasma and Knee Samples

CP Solid-phase extraction in plasma samples was performed with Discovery® DSC-18 cartridges and Visiprep DL® vacuum manifold (Supelco) followed by HPLC-UV as described by Parton et al. [12]. Knee samples were analysed as described by [13] and expressed in µg/g. The HPLC method was acceptably linear within the calibration range (0.51–103.50 µg/mL). The lower limit of quantification (LLOQ) was 0.51µg/mL.

2.5. Data Analysis. Non-Compartmental/Compartmental Pharmacokinetic/Deconvolution Analysis

Individual pharmacokinetic parameters [14] were estimated using non-compartmental analysis. The in vivo CP input rate from the nanoformulation I(t) was calculated by numerical deconvolution [15] with Phoenix-WinNonlin® 64.8.2 Certara Inc. All CP plasma concentrations (IV and IA) were simultaneously analyzed with a population approach using NONMEM ver 7.4 [16] and Xpose R package v4.2.1, as diagnostic tool. The first-order-conditional estimation method (FOCEI) with interaction was used for parameter estimation [17]. Inter-individual variability (IIV) exponentially modeled was evaluated for each pharmacokinetic parameter. Additive and combined error models were tested for residual variability. Model selection was based on: decrease in the minimum objective function (MOFV; -2xlog likelihood); parameter precision and visual inspection of goodness-of-fit plots (Gofs). A decrease in MOFV of 7.879 between nested models was statistically significant ($p <$ 0.005). For non-hierarchical models, the model with lowest Akaike criterion (AIC) was selected [18]. One- and two-open-compartment models with linear elimination parameterized as distributional clearance (CLD), apparent distribution volumes (V), and elimination clearance (CL) were fitted to the data. Allometric weight scaling was *a priori* added to all disposition parameters standardized to 70 kg body weight [19–21]. The power parameter was 0.75 for clearances and 1.0 for distribution volumes [22]. Table 1 and Figure 1 summarize tentatives of description of CP release/absorption from nanoparticles. The descriptive/predictive capability of the final model was evaluated through Gofs and visual predictive check (VPC) [23].
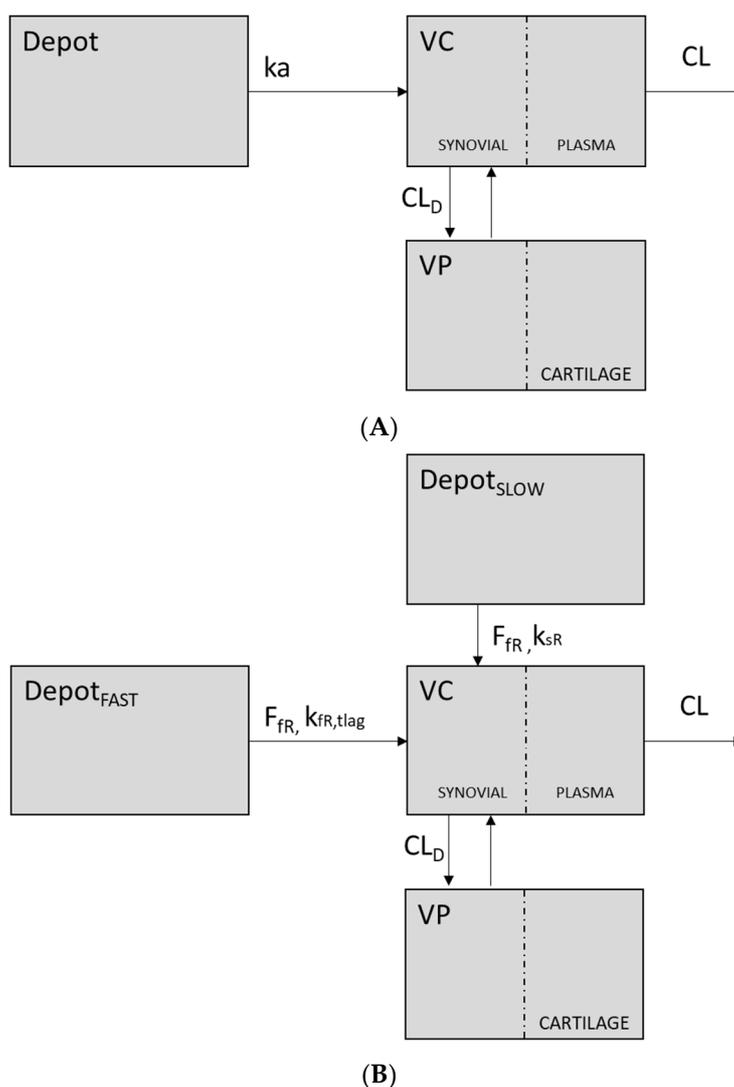

(**A**)

(**B**)

Figure 1. Schematic of the pharmacokinetic models fitted to CP concentrations achieved after IV and IA administrations. (**A**) (top): One depot release/absorption models with first or zero order rate constants (ka). (**B**) (bottom): Two depots release/absorption models CL = plasma clearance; CL_D = intercompartmental clearance between central and peripheral compartments; VC: central Distribution volume, VP: peripheral Distribution volume. K_{FR}: fisrt order initial rapid release rate constant; K_{SR}: slow release rate constant. F_{FR}: fraction of drug released during the initial fast phase; F_{SR}: fraction of drug released during the slow phase; $TlagSR$: lag-time of the slow release phase.

Table 1. Tentative models for description of CP release/absorption from nanoparticles. Models are depicted in Figure 1A (models 1–2) and Figure 1B (models 3–6).

Model	Kinetics of the Release/Absorption Process	Sequential vs. Parallel	Number of Depots
1	1st order absorption (ka)	-	one
2	Zero order absorption (ka)	-	one
3	Two 1st order absorption processes (kfr, ksr)	Parallel	two
4	1st order (kfr) and zero order absorption processes (ksr)	Parallel	two
5	1st order (kfr) and zero order absorption processes (ksr)	Sequential	two
6	Two 1st order absorption processes (kfr, ksr)	Sequential	two

3. Results

3.1. Carprofen Concentrations

Mean ± SD plasma concentrations are displayed in Figure 2. Table 2 summarizes the comparative CP concentrations in knee tissues at 9 h post-IA-administration.
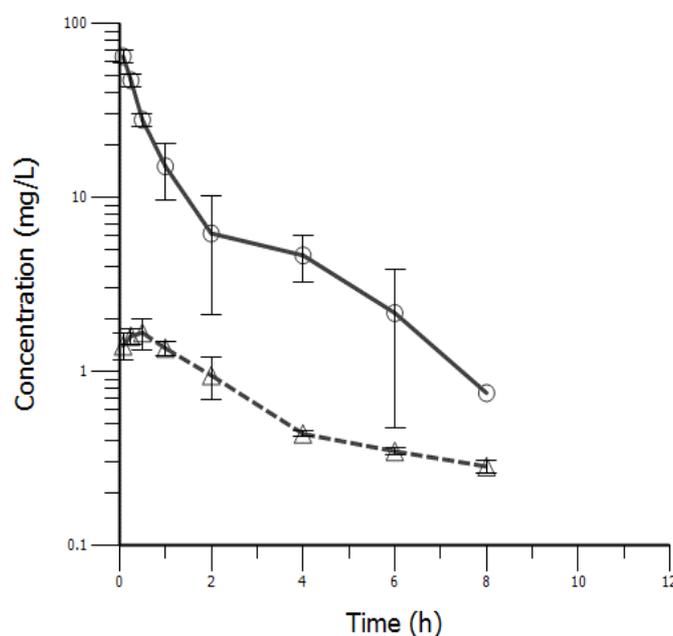

Figure 2. Overlayed individual (A: iv, B: IA) and mean ± SD (C) CP plasma concentration (mg/L) vs. time (h) profiles observed following intravenous and intraarticular administration at the doses of 4 mg/kg and 1.98 mg respectively.

Table 2. Femoral cartilage (both condyles), synovial fluid, meniscus and plasma CP concentrations at 9 h after IA administration at the dose of 1.98 mg.

Tissue	Concentration (µg/g) *
Cartilage	0.997
Meniscus	0.099
Synovial fluid	0.049
Plasma	0.3

* Once the distribution equilibrium was reached, the highest concentrations occurred in cartilage followed by meniscus, plasma and then synovial fluid.

3.2. Pharmacokinetic Analysis

Table 3 summarizes the main non-compartmental disposition/absorption parameters. Caution should be taken because the high extrapolation percentage after IA administration (>20%), suggests that release/absorption process and bioavailability (51.4%) could not be accurately characterized.

Table 3. Mean ± SD values of the main pharmacokinetic parameters estimated by the non-compartmental approach, after iv and IA administration of CP to rabbits at 4 mg/kg and 1.98 mg, respectively.

PK Parameter	Intravenous Administration	Intra-Articular Administration
λz (h^{-1})	0.3565 ± 0.1546	0.1892 ± 0.0436
$t_{1/2\lambda z}$ (h)	2.16 ± 0.76	3.78 ± 0.78
AUC (mg/L)·h	65.03 ± 20.90	6.73 ± 0.38
AUC/D	4.24 ± 1.36	3.40 ± 0.19
AUC$_{extrap}$ (%)	4.18 ± 4.06	28.29 ± 2.92
CL (L/h)	0.2533 ± 0.0831	-
V_i (L)	0.2058 ± 0.0273	-
V_{ss} (L)	0.4403 ± 0.0758	-
V_{darea} (L)	0.7963 ± 0.414	-
C_{max} (mg/L)	75.67 ± 12.40	1.84 ± 0.19
C_{max}/D	4.93 ± 0.81	0.93 ± 0.96
T_{max} (h)	-	0.25 (0.08–0.5)
F (%)	-	94.48 ± 27.83

λz: apparent elimination rate constant; $t_{1/2\lambda z}$: elimination half life; AUC: Area under the concentration vs. time curve; D: Dose in mg/kg.; AUC$_{extrap}$: Percentage of extrapolated area; CL: Plasma clearance; V_i: initial distribution volume; V_{darea}: distribution volume associated to the terminal phase; V_{ss}: distribution volume at steady-state; C_{max}; peak concentrations; T_{max}; time to peak concentration after IA administration (Median and range); F: bioavailability after IA administration, estimated as the ratio of dose normalized AUC values after IA administration to dose normalized AUC values after IV administration. Peak concentrations after the intraarticular administration were rapidly achieved (median T_{max} = 0.25 h). The higher apparent half-life after IA compared to IV, suggested a *flip-flop* phenomenon from nanoparticles, providing slower release/absorption rate than elimination process.

A total of 47 CP plasma concentrations were analysed by the population approach. Concentrations below LLOQ (23.4%) were replaced by LOQ/2. CP disposition was best described by a two-compartment model. IIV was only associated with CL. The CP release/absorption from nanoparticles consisted of two first-order processes (K_{fR}: fast and K_{sR}: slow. Thus, the IA dose was partitioned into fast (F_{fR}·F1·Dose$_{IA}$) and slow (F_{sR}·F1·Dose$_{IA}$) absorption compartments, where F_{fR} refers to the fraction of the administered dose for the fast absorption and F_{sR} to the slow absorption (F_{sR} = 1-F_{fR}). F1 and Dose$_{IA}$ the absolute bioavailabilty and the input from the IA CP dose at time of administration, respectively. The basic Gofs plots (Figure 3), and the VPC (Figure 4) confirmed the descriptive/predictive model capability. The final population pharmacokinetic parameters are shown in Table 4.
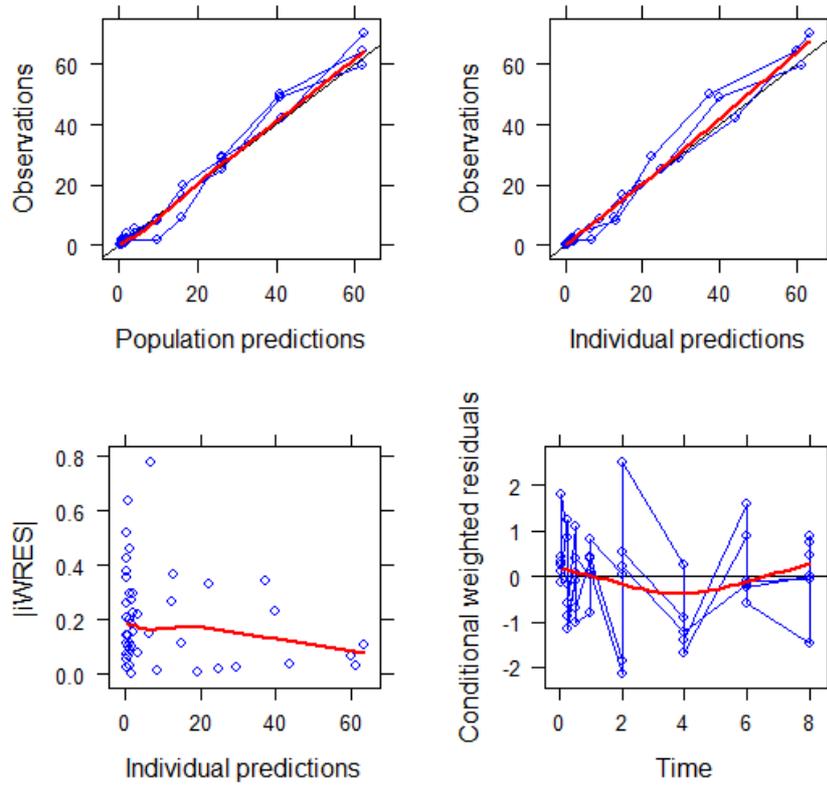
Figure 3. Goodness-of-fit plots for the population pharmacokinetic model. Superimposed values of the observed (OBS, open circles), individual predicted (IPRED, solid line) and population predicted (PRED, dashed lines) CP plasma concentrations (mg/L) vs. time (post-dosing time, h) observed in the three animals of the study after 4 mg/kg IV and 1.98 mg IA. IWRES: Individual weighted residuals; CWRES: Conditional weighted residuals. Dashed line: identity line; Solid line: Smooth line indicating the general data trend.
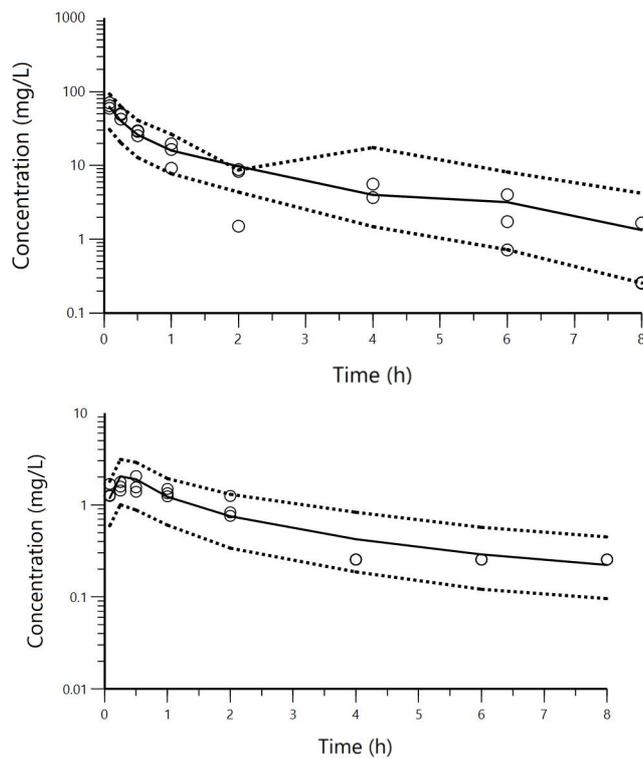
Figure 4. Predictive check of the pharmacokinetic model for CP after the IV and IA administrations. The VPCs were constructed from the fixed and random estimates obtained from the final selected model. One thousand concentration-time profiles were simulated using Monte Carlo simulations after each administration route and their non -parametric 95% confidence intervals (the 2.5th and 97.5th percentiles) were calculated and represented together with the observed data for visual inspection.

The circles represent the observed data. Dashed lines depict the 2.5th and 97.5th percentiles of the simulated concentrations. Solid line correspond to the 50th percentiles of the simulated concentrations. VPC showed that most of the data fell within the 90% prediction interval and were symmetrically distributed around the median both after iv and IA administrations.

Table 4. Mean (RSE%) values of the disposition and absorption pharmacokinetic parameters estimated by the final model.

Parameter	Units	Final Model Parameter Estimate (RSE%)
Disposition parameters		
CL	L/h·70 kg	2.00 (*8.25*)
V_C	L/70 kg	3.60 (*9.36*)
CL_D	L/h·70 kg	3.08 (*4.90*)
V_P	L/70 kg	4.28 (*14.21*)
Release/Absorption parameters		
F	%	51.4 (9.82)
Ka_{FR}	h^{-1}	7.38 (*9.17*)
Ka_{SR}	h^{-1}	0.0667 (*15.59*)
F_{FR}	%	0.595 (*1.20*)
F_{SR}	%	0.405
T_{lagSR}	h	0.5 (0.11)
Inter-individual variability		
IIV_{CL}	%	19.21 62.6)
Residual variability		
Proportional	%	25.51 (*29.34*)

CL = plasma clearance; V_C and V_P = volumes of distribution for central and peripheral compartments; CL_D = intercompartmental clearance between central and peripheral compartments; IIV and residual variability given as coefficient of variation (%). Ka_{FR}: initial rapid release rate constant; Ka_{SR}: slow release rate constant. F: Bioavailability; F_{FR}: fraction of drug released during the initial faster phase; F_{SR}: fraction of drug released during the slow phase; T_{lagSR}: lag-time of the slow phase release. All final parameter estimates are shown with the relative standard error (RSE) indicated by italic numbers in parentheses, demonstrating an acceptable precision.

Individual in vivo cumulate release/absorption and input rate I(t) profiles from the assayed IA nanoformulation are shown in Figure 5. An initial first-order kinetics burst effect was followed by a more sustained release.
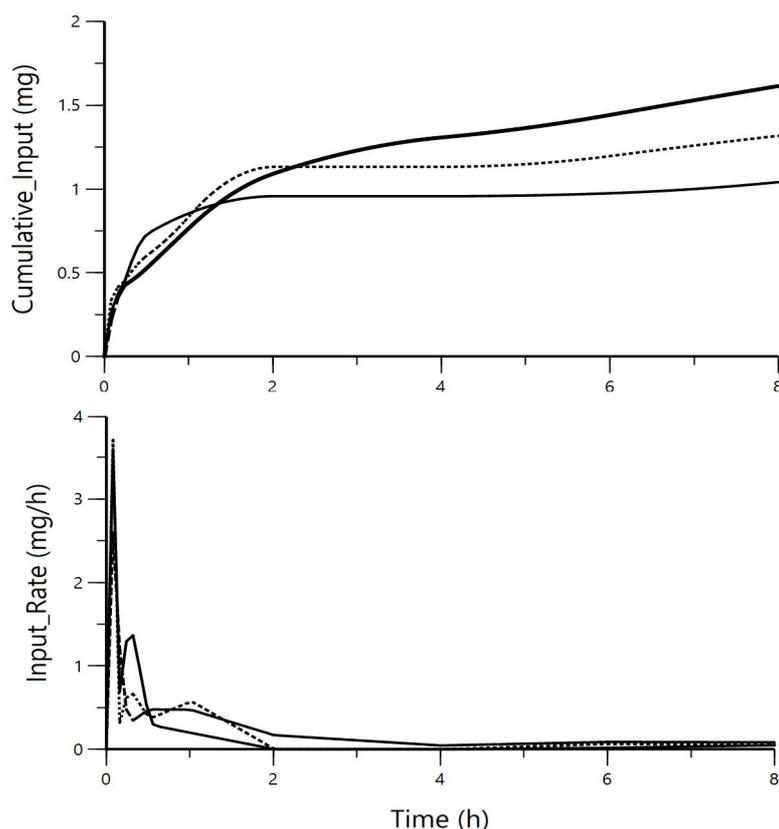
Figure 5. Individual in vivo cumulate release/absorption (up) and input rate I(t) (down) profiles of CP from the assayed IA nanoformulation. These profiles were in agreement with in vivo release/absorption pattern described by the final model. This profile resulted to be different than that observed in the in vivo evaluation assay designed for this nanoformulation resulting very useful to optimize the conditions of in vitro evaluation.

4. Discussion

Anatomical similarities of rabbits with other species (dog, cat), suggests the extrapolation of in vivo CP release/absorption to these species. As previously reported [12,24,25], CP disposition was best described by a two-compartment model. The steady-state distribution volume ($V_{ss} = 0.1126$ L/kg mean live bodyweight) was in line with other results in rabbits [26], dogs 0.1192 L/kg [24] or cats (0.1506 L/kg) [27]. Considering a total body-water of 0.61 L/kg in live rabbits [28], the low V_{ss} values suggest that carprofen is mainly confined in plasma according to its high protein-binding [29] as other NSAIDs [2].

Predicted CP clearance (1.99 L/h/70 kg) was in agreement with results in healthy volunteers [29] (100 mg IV: 2.916 L/h). However, somewhat higher CL was predicted for 7.1–15.8 kg dogs (0.0447 vs. 0.01487 L/h·kg) and for 1.9–6.0 kg cats (0.058 vs. 0.006 L/h/kg). Prediction failure of allometric CP model is probably due to large interspecies differences in metabolic patterns [22]. The metabolic pathway is only known in dogs, cat and humans [30] but not in rabbits.

The CP bioavailability from the nanoparticles (51.4%) was lower than expected, since IA route obviates first-pass effects. Analytical limitations preventing the complete characterization of the release/absorption profile (extrapolated areas > 20%), or a higher iv variability than anticipated probably due to the low number of animals can be the cause. The *flip-flop* phenomenon of IA nanoparticles support a longer residence time than conventional formulations. The CP release/absorption profile was best described by an initial burst effect (fast release component) due to the rapid release/absorption of the unencapsulated fraction into central compartment with a rate constant of 7.38 h-1 (K_{fR}) resulting in a high concentration gradient between synovial fluid and plasma at initial times. Afterwards, a sequential second process with a slower first order release rate constant

(K_{SR} = 0.0667 h-1) of microencapsulated CP occurred. The fast process contributed to the 60% of total CP reaching the systemic circulation while the slow release prevented CP from leaving the joint space rapidly. Poorly-optimized inclusion of the non-ionic surfactant beneath the PLGA matrix [31] could have contributed to such undesirable initial burst effect, so improvement of the formulation would be required to extend the CP residence time in the synovial cavity. Additionally, the reduced intraarticular volume in rabbits has demanded for the injection of a minimal volume (0.4 mL) that, although is highly concentrated to migrate towards the cartilage it does not allow to build up a relevant drug reservoir for a significant modified release. In any case, CP plasma levels resulted to be higher than IC50 for Cox2 [32] both after IV and IA administrations. The lower albumin concentrations in synovial fluid (60%) in rabbits compared to plasma resulted in higher total plasma CP concentrations than in synovial cavity once the distribution equilibrium reached, as also reported in sheep [25] and in horse [2].

The cumulative input profile predicted by deconvolution was useful to optimize previous in vitro evaluation tests. Indeed, inadequate in vitro release profiles [33] have been due to, probably, an inappropriate membrane type.

5. Conclusions

In vivo characterization of a new CP nanoformulation for IA administration has been performed in rabbits. The pharmacokinetic profile was scalable to other species. The CP burst effect inside the joint space enhances its diffusion towards cartilage and plasma. Although a limited number of animals, the rabbit model seems suitable for a predictive evaluation of the release enhancement of CP (not dued to sterical retention of the formulation) towards the biophase of arthritic diseases.

Abbreviations

The following abbreviations are used in this manuscript:

CP	Carprofen
CLD	Distributional clearence
IA	Intraarterial

References

1. Lees, P.; Aliabadi, F.S.; Landoni, M.F. Pharmacodynamics and Enantioselective Pharmacokinetics of Racemic Carprofen in the Horse. *J. Vet. Pharmacol. Ther.* **2002**, *25*, 433–448, doi:10.1046/j.1365-2885.2002.00436.x.

2. Lipscomb, V.; AliAbadi, F.; Lees, P.; Pead, M.; Muir, P. Clinical Efficacy and Pharmacokinetics of Carprofen in the Treatment of Dogs with Osteoarthritis. *Vet. Rec.* **2002**, *22*, 684–689.

3. Skjodt, N.; Davies, N. Clinical Pharmacokinetics and Pharmacodynamics of Bromfenac. *Clin. Pharmacokinet.* **1999**, *36*, 399–408, doi:10.1007/s40262-020-00868-0.

4. Zhang, Z.; Huang, G. Intra-Articular Lornoxicam Loaded PLGA Microspheres: Enhanced Therapeutic Efficiency and Decreased Systemic Toxicity in the Treatment of Osteoarthritis. *Drug Deliv.* **2012**, *19*, 255–263, doi:10.3109/10717544.2012.700962.

5. Edwards, S.H.R. Intra-Articular Drug Delivery: The Challenge to Extend Drug Residence Time within the Joint. *Vet. J.* **2011**, *190*, 15–21, doi:10.1016/j.tvjl.2010.09.019.

6. Tunçay, M.; Çaliş, S.; Kaş, H.S.; Ercan, M.T.; Peksoy, I.; Hincal, A.A. Diclofenac Sodium Incorporated PLGA (50:50) Microspheres: Formulation Considerations and in Vitro/in Vivo Evaluation. *Int. J. Pharm.* **2000**, *195*, 179–188, doi:10.1016/S0378-5173(99)00394-4.

7. Weissig, V.; Pettinger, T.K.; Murdock, N. Nanopharmaceuticals (Part 1): Products on the Market. *Int. J. Nanomed.* **2014**, *9*, 4357–4373, doi:10.2147/IJN.S46900.

8. Jiang, D.; Zou, J.; Huang, L.; Shi, Q.; Zhu, X.; Wang, G.; Yang, H. Efficacy of Intra-Articular Injection of Celecoxib in a Rabbit Model of Osteoarthritis. *Int. J. Mol. Sci.* **2010**, *11*, 4106–4113, doi:10.3390/ijms11104106.

9. Horisawa, E.; Kubota, K.; Tuboi, I.; Sato, K.; Yamamoto, H.; Takeuchi, H.; Kawashima, Y. Size-Dependency of DL-Lactide/Glycolide Copolymer Particulates for Intra-Articular Delivery System on Phagocytosis in Rat Synovium. *Pharm. Res.* **2002**, *19*, 132–139, doi:10.1023/A:1014260513728.

10. Horisawa, E.; Hirota, T.; Kawazoe, S.; Yamada, J.; Yamamoto, H.; Takeuchi, H.; Kawashima, Y. Prolonged Anti-Inflammatory Action of DL-Lactide/Glycolide Copolymer Nanospheres Containing Betamethasone Sodium Phosphate for an Intra-Articular Delivery System in Antigen-Induced Arthritic Rabbit. *Pharm. Res.* **2002**, *19*, 403–410, doi:10.1023/A:1015123024113.

11. Lentner, C. *Geigy Scientific Tables*, 8th ed.; Basel, Switzerland, 1981.

12. Parton, K.; Balmer, T.V.; Boyle, J.; Whittem, T.; Machon, R. The Pharmacokinetics and Effects of Intravenously Administered Carprofen and Salicylate on Gastrointestinal Mucose and Selected Biochemical Measurements in Healthy Cats. *J. Vet. Pharmacol. Ther.* **2000**, *23*, 73–79, doi:10.1046/j.1365-2885.2000.00253.x.

13. Parra, A.; Clares, B.; Rosselló, A.; Garduño-Ramírez, M.L.; Abrego, G.; García, M.L.; Calpena, A.C. Ex Vivo Permeation of Carprofen from Nanoparticles: A Comprehensive Study through Human, Porcine and Bovine Skin as Anti-Inflammatory Agent. *Int. J. Pharm.* **2016**, *501*, 10–17, doi:10.1016/j.ijpharm.2016.01.056.

14. Gibaldi, M.; Perrier, D. *Farmacocinética*; Reverté: Barcelona, Spain, 1982.

15. Veng-Pedersen, P. Linear and Nonlinear System Approaches in Pharmacokinetics: How Much Do They Have to Offer? I General Considerations. *J. Pharmacokinet. Biopharm.* **1988**, *16*, 413–472.

16. Bauer, R. Nonmem Users Guide Introduction To Nonmem 7.2.0. *J. Chem. Inf. Model.* **2011**, *53*, 1689–1699.

17. Hooker, A.C.; Staatz, C.E.; Karlsson, M.O. Conditional Weighted Residuals (CWRES): A Model Diagnostic for the FOCE Method. *Pharm. Res.* **2007**, *24*, 2187–2197, doi:10.1007/s11095-007-9361-x.

18. Yamaoka, T.; Nakagawa, T.; Uno, T. Application of Akaike's Information Criterion (AIC) in the Evaluation of Linear Pharmacokinetics Equations. *J. Pharmacokinet. Biopharm.* **1978**, *6*, 165–175.

19. Holford, N. The Visual Predictive Check Superiority to Standard Diagnostic (Rorschach) Plots Warfarin Predictive Check•Estimate Parameters with Warfarin Data Warfarin Turnover Lose One Dimension (Time or Prediction) Visual Check Is More Informative and Diagnost. *Pharmacology* **2005**, 92019.

20. Anderson, B.J.; Holford, N.H.G. Mechanism-Based Concepts of Size and Maturity in Pharmacokinetics. *Annu. Rev. Pharmacol. Toxicol.* **2008**, *48*, 303–332, doi:10.1146/annurev.pharmtox.48.113006.094708.

21. Anderson, B.J.; Holford, N.H.G. Mechanistic Basis of Using Body Size and Maturation to Predict Clearance in Humans. *Drug Metab. Pharmacokinet.* **2009**, *24*, 25–36, doi:10.2133/dmpk.24.25.

22. Mahmood, I. Misconceptions and Issues Regarding Allometric Scaling during the Drug Development Process. *Expert Opin. Drug Metab. Toxicol.* **2018**, *14*, 843–854, doi:10.1080/17425255.2018.1499725.

23. Bergstrand, M.; Hooker, A.C.; Wallin, J.E.; Karlsson, M.O. Prediction-Corrected Visual Predictive Checks for Diagnosing Nonlinear Mixed-Effects Models. *AAPS J.* **2011**, *13*, 143–151, doi:10.1208/s12248-011-9255-z.

24. Messenger, K.M.; Wofford, J.A.; Papich, M.G. Carprofen Pharmacokinetics in Plasma and in Control and Inflamed Canine Tissue Fluid Using in Vivo Ultrafiltration. *J. Vet. Pharmacol. Ther.* **2016**, *39*, 32–39, doi:10.1111/jvp.12233.

25. Sidler, M.; Fouché, N.; Meth, I.; von Hahn, F.; von Rechenberg, B.; Kronen, P.W. Preliminary Study on Carprofen Concentration Measurements after Transcutaneous Treatment with Vetdrop® in a Microfracture Joint Defect Model in Sheep. *BMC Vet. Res.* **2014**, *10*, 268, doi:10.1186/s12917-014-0268-6.

26. Hawkins, M.G.; Taylor, I.T.; Craigmill, A.L.; Tell, L.A. Enantioselective Pharmacokinetics of Racemic Carprofen in New Zealand White Rabbits. *J. Vet. Pharmacol. Ther.* **2008**, *31*, 423–430, doi:10.1111/j.1365-2885.2008.00975.x.

27. Taylor, P.M.; Delatour, P.; Landoni, F.M.; Deal, C.; Pickett, C.; Shojaee Aliabadi, R.; Foot, P.; LEES, P. Pharmacodynamics and Enantioselective Pharmacokinetics of Carprofen in the Cat. *Res. Vet. Sci.* **1996**, *60*, 144–151, doi:10.1111/j.2042-3306.1994.tb04370.x.

28. Panaretto, B.A. Body Composition in Vivo. I. The Estimation of Total Body Water with Antipyrine and the Relation of Total Body Water to Total Body Fat in Rabbits. *Aust. J. Agric. Res.* **1963**, *14*, 594–601.

29. Crevoisier, C. Pharmacokinetic Properties of Carprofen in Humans. *Eur. J. Rheumatol. Inflamm.* **1982**, *5*, 492–502.

30. Ray, J.E.; Wade, D. The Pharmacokinetics and Metabolism of 14C-Carprofen in Man. *Biopharm. Drug Dispos.* **1982**, *3*, 29–38.

31. Morille, M.; Van-Thanh, T.; Garric, X.; Cayon, J.; Coudane, J.; Noël, D.; Venier-Julienne, M.C.; Montero-Menei, C.N. New PLGA-P188-PLGA Matrix Enhances TGF-B3 Release from Pharmacologically Active Microcarriers and Promotes Chondrogenesis of Mesenchymal Stem Cells. *J. Control. Release* **2013**, *170*, 99–110, doi:10.1016/j.jconrel.2013.04.017.

32. Miciletta, M.; Cuniberti, B.; Barbero, R.; Re, G. In Vitro Enantioselective Pharmacodynamics of Carprofen and Flunixin-Meglumine in Feedlot Cattle. *J. Vet. Pharmacol. Ther.* **2014**, *37*, 43–52, doi:10.1111/jvp.12052.

33. Parra, A.; Mallandrich, M.; Clares, B.; Egea, M.A.; Espina, M.; García, M.L.; Calpena, A.C. Design and Elaboration of Freeze-Dried PLGA Nanoparticles for the Transcorneal Permeation of Carprofen: Ocular Anti-Inflammatory Applications. *Colloids Surfaces B Biointerfaces* **2015**, *136*, 935–943, doi:10.1016/j.colsurfb.2015.10.026.

Publisher's Note: MDPI stays neutral with regard to jurisdictional claims in published maps and institutional affiliations.